

Characterization of dissolving pulp by multivariate data analysis of FT-IR and NMR spectra

Peter Strunk, Tommy Öman, András Gorzsás, Mattias Hedenström and Bertil Eliasson

KEYWORDS: Cellulose, Dissolving pulp, Hemicelluloses, FT-IR spectroscopy, Multivariate data analysis, NMR spectroscopy, Pulp viscosity, Wood type

SUMMARY: Several grades of dissolving pulps have been analyzed using FT-IR, solid state ^{13}C NMR and two dimensional ^1H - ^{13}C HSQC NMR spectroscopy to obtain an extensive data set for further characterization. The selection of the dissolving pulps with high cellulose purity was based on pulping process, wood type and, intrinsic pulp viscosity. Multivariate data analysis was used to investigate how information derived from the spectroscopic data correlate to each of the selection criterion: wood type, process type and viscosity. The spectroscopic methods were also compared with common dissolving pulp analyses to see to what extent spectroscopy can predict pulp analyses.

Correlations were found between the spectroscopic data and the pulp characteristics process type and wood type, but not for intrinsic viscosity. A reason for a good correlation to wood type appears to be the hemicelluloses composition, expressed as the xylose:mannose ratio by 2D NMR spectroscopy. For process type, 2D NMR showed the most characteristic property to be the amount of reducing ends in the cellulosic samples, which in turn strongly correlates to lower molecular weight for the sulfite samples as determined by molecular weight distribution.

Many common, yet expensive and time consuming, pulp analyses could also be predicted by the achieved models. It can be concluded that investigations of dissolving pulp characteristics, especially concerning different wood and process types, can take advantage of the methods and models presented in this study.

ADDRESSES OF THE AUTHORS: Peter Strunk (peter.strunk@chem.umu.se), Tommy Öman (tommy.oman@chem.umu.se), Mattias Hedenström (mattias.hedenstrom@chem.umu.se) and Bertil Eliasson (bertil.eliasson@chem.umu.se): Department of Chemistry, Umeå University, SE-901 87 Umeå, Sweden, András Gorzsás (andras.gorzsas@genfys.slu.se), Department of Forest Genetics and Plant Physiology, Swedish University of Agricultural Sciences (SLU) S-901 83 Umeå, Sweden

Corresponding author: Peter Strunk

Abbreviations:

DP: Degree of polymerization.

FT-IR: Fourier transform infrared spectroscopy.

MVDA: Multivariate data analyses.

Mv: Viscosity average molecular mass.

Mw: Weight average molecular mass.

Mn: Number average molecular mass.

OPLS-DA: Orthogonal projection to latent structures with discriminant analysis.

PCA: Principal component analysis.

PD: Polydispersity (molecular weight distribution).

PLS: Partial least squares regression.

Q^2 : Validation of model, goodness of prediction.

R10, R18: Weight proportion of cellulosic residue in 10% and 18% NaOH solution.

2D ^1H ^{13}C HSQC NMR: Two dimensional hetero-nuclear single quantum coherence nuclear magnetic resonance.

The production and market share of dissolving pulp of the total global pulp production is steadily increasing due to a higher demand of sustainable products and cellulosic fibers, promoted by an increasing world population and a decreasing cotton production (KGI 2009). Dissolving pulps – characterized by lower hemicelluloses content compared to paper grade pulps and higher reactivity towards alkali and other chemicals – are widely used when manufacturing cellulose derivatives, microcrystalline cellulose for pharmaceutical use and regenerated cellulose. There is a wide array of dissolving pulps available on the market, with specific characteristics depending on the choice of wood type and pulping process for manufacturing these pulps. The refinement process of dissolving pulps to a specific derivative is intrinsically dependent on these characteristics, and knowledge about the pulp properties is thus important (Strunk et al. 2011). Many methods for the characterization of the properties of dissolving pulp are available and used today. Common analyses include metal and carbohydrate content, intrinsic viscosity, brightness and alkali resistances such as R10 and R18. However, most of these analytical methods are time consuming and costly. It is thus of great interest to find faster and simpler ways to replace or complement some of the wet chemical analyses by spectroscopic methods provided that the same accuracy can be obtained.

FT-IR spectroscopy has today widespread use in the pulp and paper industry, ranging from off-line applications in the laboratory (characterization of lignocellulosic material, extractives, contaminants, additives, etc) to on-line process control. A thorough overview of this field has been given by Leclerc and Trung (2002). Apart from the industrial applications, basic scientific analyses also apply FT-IR frequently to study lignocellulosic materials, for

instance with the purpose to explain structural features of cellulose (Zhbakov et al. 2005). It is a versatile, non-destructive technique that can probe various compositional changes in pulp samples with minimum to no sample destruction, especially in attenuated total reflectance (ATR) mode. Even though ATR FT-IR has only a thin depth of penetration of the IR beam into the sample such as near infrared spectroscopy (NIR), it is when coupled with multivariate analysis a powerful tool to analyse differences among various classes of pulp samples.

Solid-state ^{13}C NMR spectroscopy has been used extensively for cellulose and pulp analysis and is particularly useful for the analysis of cellulose crystallinity (Wickholm et al. 2001; Hult et al. 2000; Iversen et al. 2000; Larsson et al. 1999; Atalla et al. 1980; Isogai et al. 1989; Kunze et al. 1983). We also employed the newly developed method for analysis of wood material in solution using two-dimensional ^1H - ^{13}C HSQC NMR experiments (Kim et al. 2008; Lu, Ralph 2003). This method has been shown to yield a detailed chemical fingerprint of all major secondary cell wall components where both the chemical structure and the relative amounts of cellulose, hemicelluloses and lignin can be determined. In a previous study of tension wood, we combined 2D HSQC spectra and multivariate analysis to study changes in both carbohydrate and lignin composition (Hedenström et al. 2009).

The dissolving pulps used in this study were obtained from five different manufacturers, and originated from different pulping processes and different wood types. Two or three viscosity grades from each producer were also included. FT-IR, solid-state ^{13}C NMR and solution 2D ^1H - ^{13}C HSQC NMR spectroscopy were used to get information about the chemical composition of the pulp samples. The spectral data obtained were treated by means of multivariate data analysis to correlate differences in the dissolving pulp samples to the choice of raw material (softwood, SW or hardwood, HW), process type (sulfate or sulfite) and pulp viscosity. It was also investigated whether the derived models could be used to obtain information on cellulose properties given today by expensive and time consuming, conventional methods. For this purpose, a number of wet chemical analyses (see experimental part) were undertaken and the results are reported.

Hence, the central questions of this study have been *i*) if the origin of a sample of dissolving pulp can be determined by one or all of the three spectroscopic methods, *ii*) if some of the chemical and physical properties given by conventional analysis methods could be predicted, and *iii*) if further information about the pulps not covered by these conventional methods could be revealed.

Materials and Methods

Dissolving pulps were chosen by process type (sulfate and sulfite) as well as wood type (softwood or hardwood). For each sample, a high and a low commercially available viscosity was chosen, ranging from 420 to 850 ml g^{-1} . These viscosities correspond to a degree of polymerization (DP) of 574 and 1250, respectively, using the formula $\text{DP}^{0.9055} = 0.75 \times (\text{intrinsic viscosity, ml g}^{-1})$ (Immergut et al. 1953). Hence, the conditioning factors were established with two qualitative (process type and wood type) and one quantitative factor (viscosity). The samples were provided by 5 different producers, but no low-viscosity sample from producer A was available. A sample with intermediate viscosity from producer B was also included. Even though producers B and C represent similar samples regarding the applied design factors, samples from both manufacturers were included to evaluate differences between them. In total, this resulted in a set of ten pulp samples (*Table 1*).

Chemical analysis

For each of the selected dissolving pulps, chemical analyses such as viscosity and alkali resistance with 18% sodium hydroxide (R18) as well as with 10% sodium hydroxide (R10) were performed. Pulp viscosity was measured using a capillary tube viscometer according to ISO 5351/1-1981 whereas alkali resistance was measured according to ISO 699.

Carbohydrate composition

The carbohydrate composition was determined at MoRe Research laboratories in Örnköldsvik, Sweden, by a company internal method. All pulps were pre-hydrolyzed with 72% sulfuric acid for one hour in a 30°C water bath after which the samples were hydrolyzed in an autoclave for 1 hr at 120°C. The solution was then neutralized with sodium hydroxide and transferred into a Dionex DX500 ion chromatograph equipped with a GP40 gradient pump, a CarboPac PA1 pre-column and analytical column, and a pulsed ED40 amperometrical detector. Gradient elution was carried out with deionized water and a mixture of 200 mM sodium hydroxide and 170 mM sodium acetate at 1 ml min^{-1} . The sum of the hemicelluloses was determined from the amount of xylose, mannose, galactose and arabinose derived from this method.

Molecular weight distribution

All samples were activated by adding DMAc (N,N-dimethylacetamide) and were dissolved by a mixture of LiCl (lithium chloride) in DMAc

Table 1. Physicochemical properties of dissolving pulp samples.

| Sample | Producer | Wood type | Process ^a | Viscosity (ml g ⁻¹) | PD | Mw (g mol ⁻¹) | Mn (g mol ⁻¹) | R10 (%) | R18 (%) | Glucose (g kg ⁻¹) | Xylose (g kg ⁻¹) | Mannose (g kg ⁻¹) | Tot hemip ^b (g kg ⁻¹) |
|--------|----------|---------------------|----------------------|---------------------------------|------|---------------------------|---------------------------|---------|---------|-------------------------------|------------------------------|-------------------------------|--|
| 1 | A | HW (Beech) | Sulfite, Mg | 587 | 12.2 | 485500 | 39647 | 88.3 | 93.1 | 906 | 41.9 | 8.8 | 50.7 |
| 2 | B | SW (Spruce, Pine) | Sulfite, Na | 465 | 7.9 | 397154 | 50075 | 89.1 | 95.4 | 914 | 16.1 | 16.3 | 32.4 |
| 3 | B | SW (Spruce, Pine) | Sulfite, Na | 573 | 8.0 | 383647 | 47922 | 89.4 | 94.7 | 925 | 17.4 | 19.3 | 36.7 |
| 4 | B | SW (Spruce, Pine) | Sulfite, Na | 845 | 9.0 | 520837 | 57961 | 91.4 | 94.2 | 896 | 33.8 | 22.5 | 56.3 |
| 5 | C | SW (Spruce) | Sulfite, Ca | 423 | 6.9 | 354086 | 51650 | 87.3 | 95.1 | 920 | 21.5 | 10.1 | 31.6 |
| 6 | C | SW (Spruce) | Sulfite, Ca | 785 | 8.0 | 477154 | 59647 | 91.8 | 95.1 | 931 | 26.8 | 17.3 | 44.1 |
| 7 | D | HW (Eucalyptus) | Sulfate, PHK | 516 | 4.6 | 358058 | 78542 | 95.2 | 98.2 | 946 | 15.3 | 2.4 | 17.7 |
| 8 | D | HW (Eucalyptus) | Sulfate, PHK | 609 | 4.8 | 514295 | 106288 | 95.6 | 98.2 | 942 | 17.7 | 2.0 | 19.7 |
| 9 | E | SW (Pine) | Sulfate, MK | 419 | 5.8 | 292104 | 50368 | 87.1 | 90.5 | 873 | 70.2 | 56.5 | 130.6 ^c |
| 10 | F | SW (Pine, Loblolly) | Sulfate, K | 794 | 8.0 | 483635 | 60448 | 86.8 | 87.7 | 815 | 86.1 | 68.8 | 163.1 ^c |

^a For the sulfite process, the cation used is indicated. The type of sulfate process is indicated by PHK (prehydrolysis Kraft), MK (Modified Kraft) or K (Kraft).

^b Total amount of hemicelluloses, expressed as sum of xylose and mannose unless specified otherwise.

^c Contains traces of arabinose and galactose.

(Berthold et al. 2004, Sjöholm 1999) with the following modifications. A 25 mg portion of each pulp was solvent exchanged three times with 5 ml of methanol for 30 minutes followed by three times for 30 minutes with DMAc. The excess of DMAc was then removed after which 5 ml of 8w% LiCl in DMAc and 0.6 ml of the derivatizing reagent ethyl isocyanate was added and left over night at room temperature with gentle stirring. No filtration of the samples was required. The dissolved cellulose samples were then chromatographed with a Polymer Laboratories PL-GPC 210 instrument, having a 100 microliter injection loop and three size exclusion PL-Gel microM Mixed B chromatography columns with a guard column, an internal refractive index detector and a HPLC compact pump model 2250 provided by Bischoff. The flow rate for the 0.5w% LiCl in DMAc eluent was set to 1 ml min⁻¹ at a temperature of 70°C. For calibration, a standard solution of Pullulan Polysaccharide SAC-10/10 supplied by Polymer Laboratories Ltd. was used with a molecular weight of 788, 404, 212, 112, 47.3, 22.8, 11.8 and 5.9kD. Data acquisition and calculation was performed by the software Cirus 3.0, provided from Polymer Laboratories.

The polydispersity (PD), expressed by the ratio of the weight-averaged molecular weight (Mw) and the number-averaged molecular weight (Mn) of each sample, is shown in *Table 1*.

Mercury porosimetry

A Micromeritics AutoPoreIV 9500 mercury porosimeter was used to determine median pore diameter, total pore area and permeability (Byström et al. 2010). All samples were analyzed using a 3 cm³ powder penetrometer with a stem volume of 1190 mm³. Each sample had an average weight of total 1 g and was cut in smaller pieces to fill the stem. The number of recorded data points was 49 during intrusion and 31 during extrusion. An evacuation pressure of 6.7 mPa and a maximum mercury pressure of 413 MPa was applied. Three analyses per sample were performed.

FT-IR measurements

A minimum of three separate pieces in size of 1 cm² were cut from each pulp sheet and spectra were recorded using a Bruker Equinox 55 spectro-meter equipped with a diamond attenuated total reflection (ATR) accessory (SensIR Technologies Dansbury, Connecticut, USA). The sample chamber was continuously flushed with dry air. Spectra were recorded using 32 scans covering the 400 - 4000 cm⁻¹ region (mid-IR) at a 4 cm⁻¹ spectral resolution. For analysis, only the region 400 - 1500 cm⁻¹ was used to avoid contributions from remaining atmospheric intrusion and moisture. Hence, FT-IR plots show loadings from 400 to 1500 cm⁻¹. A four-point linear baseline correction (with baseline points at 400, 780, 1180 and 1500 cm⁻¹ and linear connection

between these points) and area normalisation (total sum normalisation, setting the area under all peaks in the 400-1500 cm^{-1} to unity) was also performed over this region according to a previous study (Stenlund et al. 2008).

NMR measurements

2D NMR

Sample preparation for 2D NMR was performed according to a previously published acetylation procedure (Hedenström et al. 2009, Lu, Ralph, 2003). Approximately 200 mg of dissolving pulp was ground in a 50 ml ZrO_2 jar with 10 x 10 mm ZrO_2 ball bearings using a Fritsch Pulverisette 7 model planetary ball-mill, for 90 min using 10 min milling intervals with 10 min breaks in between to avoid excessive heating of the sample. DMSO (1.8 ml) and N-methylimidazole (NMI, 900 μl) were added to 100 mg of each ball-milled sample. The samples were stirred for 24 h. Acetylation was accomplished by adding acetic anhydride (450 μl) and stirring for 1.5 h. The acetylation reaction was quenched by pouring the acetylated cell wall solution into water (600 ml), where the sample was left to precipitate for 3 h. The samples were then centrifuged in a JA-14 rotor at 10000 \times g for 10 min. The samples were washed twice following centrifugation under the same conditions. All samples were lyophilized in order to remove remaining solvents. Approximately 100 mg of each acetylated sample was dissolved in 600 μl CDCl_3 . 2D ^{13}C - ^1H HSQC spectra were acquired on a 600 MHz Bruker DRX spectrometer equipped with a 5 mm TXI triple-resonance cryoprobe with z-gradients. Adiabatic pulses were used to remove off-resonance effects. Sweep widths of 8 (^1H) and 140 (^{13}C) ppm were used and experiment time for each spectrum was approximately 2.5 h. Spectra were processed using a gaussian window function followed by baseline correction and manual phase correction. After processing, a data matrix with a size of 1024 \times 512 for each spectrum was obtained. In-house Matlab scripts (available on request) were used to prepare the data for multivariate analysis. This preparation includes selection of the spectral region of interest (2.8-6.5 ppm in the ^1H -dimension and 48-115 ppm in the ^{13}C -dimension), exclusion of data points below a noise threshold, normalization of the selected spectral region and reshaping each spectrum to a row vector. A more thorough explanation of this procedure is given elsewhere (Hedenström et al. 2009; Hedenström et al. 2008).

CP/MAS NMR

Samples for solid-state CP/MAS ^{13}C NMR were prepared by shearing approximately 1 cm^2 pieces of

cellulose with a rotor mill (Ultra Centrifugal Mill ZM 200, Retsch Inc equipped with a 0.5 mm sieve. The samples were then moisturized with 50% water (w/v) and packed into a 4 mm rotor. A Bruker DRX 500 MHz spectrometer was used for acquisition of spectra. Spinning rate was 5 kHz and 4096 scans were added, resulting in an experiment time of about 2.5 hours. A Gaussian window function was used prior to the Fourier transform, followed by manual baseline and phase corrections. Processing was performed using Topspin 2.0 (Bruker Biospin, Rheinstetten, Germany). Processed spectra were imported into Matlab and placed in a matrix suitable for multivariate analysis. Two technical replicates were analyzed for one pulp sample, resulting in 12 spectra in total.

Multivariate data analysis

Multivariate analysis of spectral data was performed in SIMCA-P+ v.12.0 (Umetrics AB, Umeå, Sweden). The methods used were principal component analysis (PCA) (Wold et al. 1987; Jackson et al. 1991) and orthogonal projection to latent structures (OPLS) (Trygg, Wold 2002), which is an extension of the partial least squares regression method (PLS) (Gerlach et al. 1979). PCA is a projection method that describes the systematic variation in a data table \mathbf{X} with a few latent variables (principal components) called scores, \mathbf{T} (Eq 1). \mathbf{E} represents the residual variation in \mathbf{X} . The weight of each original variable in the latent variables are called loadings, \mathbf{P} , and can thus be used to interpret, for example, groupings seen in the score space. PCA was here used to get an overview of the spectral data, detect outliers and groupings of samples and also to interpret some of the observed groupings.

$$\mathbf{X} = \mathbf{TP}^T + \mathbf{E} \quad [1]$$

PLS works in a similar fashion but instead of describing the largest variation within the data, the direction of the latent variables are related to a \mathbf{Y} -matrix (response matrix) which means that systematic variation in \mathbf{X} correlated to a specific response can be investigated. In contrast to PLS, OPLS divides the systematic variation in two blocks, one that is correlated to \mathbf{Y} , called predictive components \mathbf{T}_p and one that describes systemic variation orthogonal to \mathbf{Y} , \mathbf{T}_o , Eq 2. This simplifies the interpretation of the models as only the loadings along the predictive component, \mathbf{P}_p , needs to be analyzed for each response.

$$\mathbf{X} = \mathbf{T}_p\mathbf{P}_p^T + \mathbf{T}_o\mathbf{P}_o^T + \mathbf{E} \quad [2]$$

OPLS can also be used for discriminant analysis (DA) to investigate differences between the classes

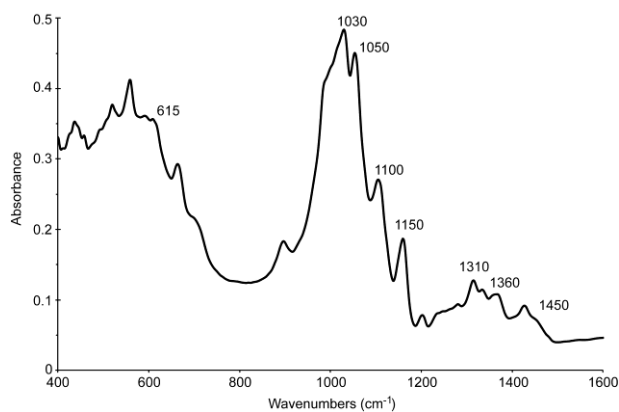


Fig 1. FT-IR spectrum of sample 8, showing the spectral range 400 – 1600 cm^{-1} , prior to baseline correction and normalization to illustrate quality. Some of the bands used in the analysis (see running text) are highlighted for clarity.

of samples and where \mathbf{Y} describes the class belonging. OPLS-DA was in this study used to correlate variation in the spectral data to the production parameters wood type and process type. Mean-centered data were used for the PCA models and UV-scaled data (each variable is centered and scaled to unit variance where the base weight is computed as $1/\text{sd}$, with sd being the standard deviation of one variable computed around the mean) were used for the OPLS-DA models. Cross-validation was used to calculate the predictive ability, Q^2 , of the models. Generally, a $Q^2 > 0.5$ is regarded as good and a $Q^2 > 0.9$ as excellent (Eriksson et al. 2006).

Results and Discussion

FT-IR analysis

A representative FT-IR spectrum from one sample (nr 8, Table 1) in the range of 400 to 1600 cm^{-1} is shown in Fig 1.

PCA model

A PCA model calculated on all spectra, base line adjusted and normalized, did not indicate any outliers and all spectra were subsequently included in the following analysis.

OPLS-DA model on process type

An OPLS-DA model where the samples were classified according to process type (sulfite or sulfate) resulted in a model with high predictability ($Q^2 = 0.93$), see Fig 2a. The corresponding loadings (Fig 2c) revealed increased band intensities (positive peaks) for the sulfate class at 810, 870, 1030, 1050 and ca 1150 cm^{-1} , which also correspond to major peaks or peaks on shoulders of larger absorptions in the FT-IR spectra.

Bands at 810 and 870 cm^{-1} are not typical in spectra of cellulose but may be assigned to hemicelluloses (Kačuráková et al. 2000), and have been attributed to glucomannan in a study of wood samples from

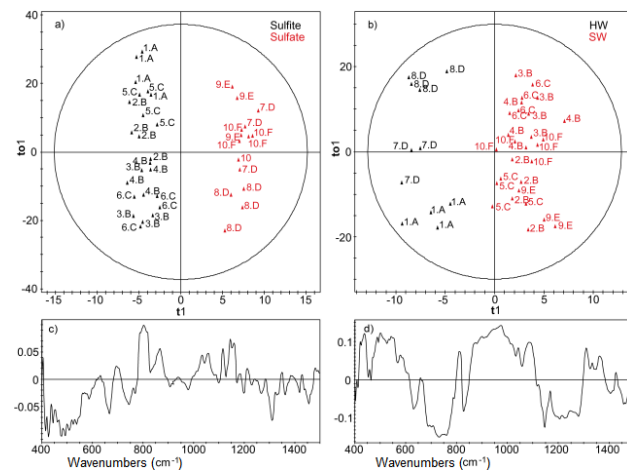


Fig 2. Plots from OPLS-DA models, obtained from FT-IR data where samples were classified according to either process type or wood type. Sample number and producer are indicated for each sample according to Table 1. (a) Score plot from a UV-scaled OPLS-DA, with samples classified to either the sulfate or sulfite process. (b) Score plot from a UV-scaled OPLS-DA where samples were classified to wood type, hardwood (HW) and softwood (SW). (c) Loading plot for the predictive component in (a). (d) Loading plot for the predictive component in (b).

Norway spruce (Åkerholm, Salmén 2001). The bands at 1030 and 1050 cm^{-1} likely arise from C-OH or in-ring C-O stretchings in the polysaccharides, while that at 1150 cm^{-1} is attributed to the asymmetric C-O-C stretch of the glycosidic link in cellulose (Maréchal, Chanzy 2000; Barsberg 2010) and in hemicelluloses (Kačuráková et al. 2000). Conversely, peaks more intense in the spectra of the sulfite-process samples comprise of those at 509, 667, 740, 1310 and 1450 cm^{-1} . Most of these bands are small and severely overlap with others. They can be assigned to cellulose although hemicelluloses have also been reported to produce bands (Labbé et al. 2005; Naumann et al. 2005) that would overlap with some of them. Although samples 9 and 10 showed a relatively high content of xylose and mannose (Table 1), a larger proportion of hemicelluloses for the sulfate processed pulp is not a sufficient reason for the model separation since samples 7 and 8 have comparatively low amounts of those carbohydrates.

OPLS-DA model on wood type

A second OPLS-DA model with sample classification into type of wood also showed a good separation of the two groups ($Q^2 = 0.76$), see Fig 2b. As the corresponding loadings reveal (Fig 2d), peaks more intense in softwood include those at 438, 500-545, 810, 875-1050, 1084, 1308 and 1360 cm^{-1} . The presence of an 810 cm^{-1} band may indicate hemicelluloses as one reason for the grouping as in the previous model, but it is apparent that additional explanations are needed since not all softwood samples have high hemi-celluloses content (see Table 1).

The bands more intense in the FT-IR model of hardwoods include those at 630, 690-760, 1150 and 1200-1280 cm^{-1} . Absorptions in this latter region may be due to O-H and C-H deformations (Siroky 2010), the symmetric C-O-C stretch of the glycolidic link (Maréchal, Chanzy 2000), and possibly vibrations in COO groups in xylan (Åkerholm, Salmén 2001) and in acetyl groups in glucomannan. However, none of the samples had detectable absorptions in the original spectra at 1725-1735 cm^{-1} , which would be expected for the carbonyl stretch modes in xylan and glucomannan (Mohebbi 2008). Therefore, the band 1200-1280 cm^{-1} does not seem to have significant contribution from hemicelluloses.

As often found in multivariate data analyses, these two OPLS studies of IR data cannot pinpoint a single property of the pulps that explain why the models distinguish between pulps from sulfite and sulfate process types, as well as hardwood and softwood. However, one may get indications about what variables are important for describing the data set. In the two present cases, the hemicelluloses content appears to be of some significance.

An investigation of the spectral profiles with regard to viscosity did not show any correlation between differences in the FT-IR spectra and differences in viscosity.

To obtain additional information from IR spectroscopy with the objective to explain the MVDA models in terms of the hemicelluloses content, the degree of crystallinity and the cellulose I/II ratio, the spectral region would have to be extended to ca. 3500 cm^{-1} (OH stretch), which was excluded from our study due to interference of atmospheric water vapour.

Solid-state ^{13}C NMR analysis

As described in the introduction, solid state ^{13}C NMR spectroscopy can be utilized for the analysis of cellulose morphology. A representative solid state ^{13}C NMR spectrum of one of the dissolving pulps is shown in *Fig 3d*.

PCA model

A PCA with the peak-intensity matrix (see Materials and Methods) was performed as a first step to get an overview of the data and also to interpret differences between the different dissolving pulps (Elg-Christoffersson et al. 2002). No outliers could be detected but it is interesting to note that the major source of variation stems from the producer rather than from the raw material or process type. The score plot (*Fig 3a*, where the subscripts cr and am denote crystalline and amorphous, respectively) from the centered PCA shows the two biggest

principal components describing 71.8% of the variation in the data (60.8% in the first component and 11% in the second). Along the first component, \mathbf{t}_1 , samples 9 and 10 differ the most from the mean and have more of the negative peaks and less of the positive peaks in the corresponding loading plot, \mathbf{p}_1 (*Fig 3b*). The positive peaks with the largest contributions to the model are the cellulose peaks with ppm values of 105.0 (C_1), 88.8 ($\text{C}_{4\text{cr}}$), 74.9 ($\text{C}_{2,3,5}$) and 72.4 ($\text{C}_{2,3,5}$). The negative peaks in the same loading plot are located at 101.75, 81.2, 78.8, 77.2, 63.6, 60.3 and 59.5 ppm and are contributions from different hemicelluloses. It could thus be concluded that samples 9 and 10 have higher hemicelluloses content, which is in agreement with the chemical analysis presented in *Table 1*.

The variation along the second component, \mathbf{t}_2 , can be interpreted with the corresponding loading vector, \mathbf{p}_2 (*Fig 3c*). Positive peaks in this loading plot are more intense for observations with high values along \mathbf{t}_2 in *Fig 3a*, for example samples 5 and 8 while the negative peaks have higher intensity for samples with negative score values along \mathbf{t}_2 , most notably sample 1. The positive peaks are located at 105.8, 88.8, 75.0, 71.5 and 65.1 ppm. The peak at 71.5 ppm might be from a hemicellulose, and the chemical shifts of the remaining positive peaks are in good agreement with literature values found for one of the crystalline cellulose structures, namely cellulose I (Atalla et al. 1980; Isogai et al. 1989; Kunze et al. 1983). Negative peaks in the loading plot are positioned at 107.7, 84.0, 76.9, 73.0 and 70.1 ppm.

The peak at 84.0 ppm may be assigned to C4 in amorphous cellulose, and the chemical shift of the peak at 107.7 ppm is in good agreement with published values for cellulose II (Dudley et al. 1983; Kono, Nomata 2004). Also the peaks at 76.9 and 73.0 ppm are most likely an indication of cellulose II although the difference in overall cellulose crystallinity makes this spectral area more difficult to interpret. The expected negative peak at 63 ppm (Vanderhart and Atalla 1984) that also would be an indication of cellulose II could not be observed, most likely because of overlap with the intense cellulose I C6 resonances in this spectral region. The peak at 70.05 ppm could not be assigned to a specific structure. From these results, it can be concluded that sample 1 has a lower degree of crystallinity and also a higher amount of cellulose II than the other dissolving pulp samples. To summarize, PCA reveals differences both in the hemicelluloses content and cellulose morphology between the different dissolving pulps. These differences could not be traced back to the design

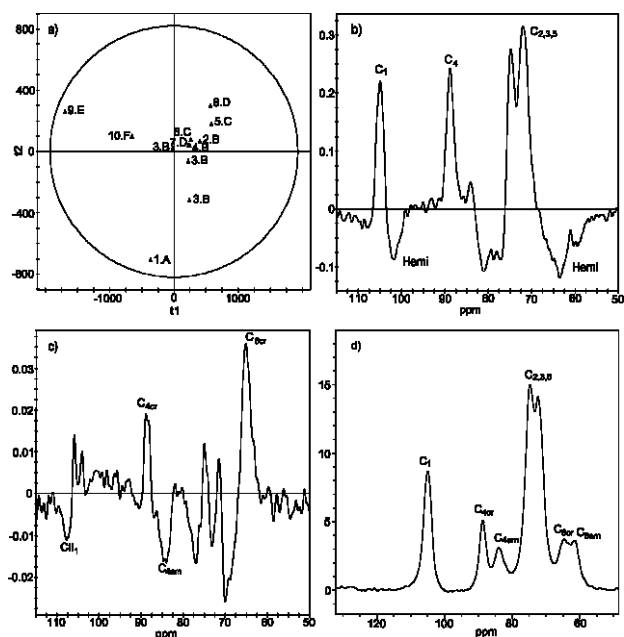


Fig 3. PCA model plots calculated from solid state ^{13}C NMR data. Samples are annotated according to table 1. Peaks from crystalline and amorphous cellulose are denoted cr and am, respectively. CII1 refers to carbon 1 in cellulose II. (a) t_1 - t_2 score plot from a mean centered PCA model. (b) Loading plot of the first component, p_1 . (c) Loading plot of the second component, p_2 . (d) A typical solid state ^{13}C NMR spectrum from dissolving pulp with cellulose assignment. C₁-C₆ represents the different carbons in the glucose unit.

parameters (wood type and process type) but are instead related to specific producers. This implies that the specific production parameters for each production site have a large impact on the final composition of the dissolving pulps.

OPLS-DA on process type, wood type and viscosity

An OPLS-DA model with process type as discriminant reveals differences in the hemicelluloses composition, see Table 2. However, differences in cellulose crystallinity could not be correlated to any process parameter. This was not unexpected considering that only sample 1 shows significant difference from the others regarding cellulose crystallinity/morphology in the PCA model. Differences in hemicelluloses composition are more suitably studied with 2D-NMR in solution, see below, since there is a large amount of overlap in the regions where hemicelluloses signals appear in the solid-state ^{13}C NMR spectra. No models for viscosity or wood type as discriminants could be obtained.

2D NMR analysis

PCA model

A PCA was performed on the 2D NMR spectra, and relevant plots from the model are shown in Fig 4. A typical 2D NMR spectrum from one of the pulp samples is shown in Fig 4d, as a reference. The first two components describe 84.6% of the variance in the spectral data. The score plot (Fig 4a) shows

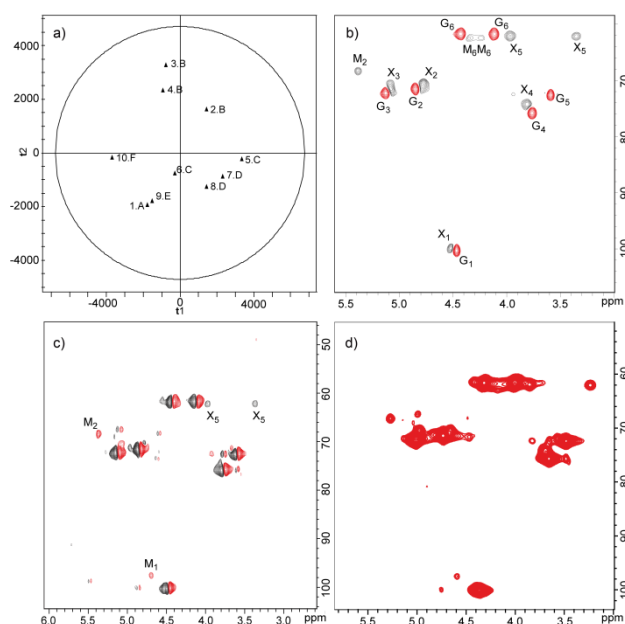


Fig 4. PCA model calculated from 2D ^1H - ^{13}C HSQC NMR data. (a) t_1 - t_2 score plot from a mean centered PCA model. (b) Loading plot for the first component, p_1 . (c) Loading plot for the second component, p_2 . G = glucose, X = xylose and M = mannose. Positive loadings are shown in red and negative in black. (d) Typical 2D ^1H - ^{13}C HSQC spectrum from sample 3 as an example.

that the sample origin, with respect to producer, is an important discriminant in the PCA, as also found by the solid-state ^{13}C NMR analysis. In the loading plot derived from the first component, Fig 4b, we observe peaks which can be ascribed to glucose (G), xylose (X) and mannose (M).

Positive peaks (in red) are assigned to glucose units and appear at $^1\text{H}/^{13}\text{C}$ ppm values of 3.59/72.6 (G_5), 3.76/75.9 (G_4), 4.12/61.7 (G_6), 4.43/61.9 (G_6), 4.46/100.2 (G_1), 4.85/71.5 (G_2) and 5.13/72.4 (G_3). Negative peaks (in black) at 3.35/62.1 (X_5), 3.82/74.3 (X_4), 3.96/62.1 (X_5), 4.52/99.8 (X_1), 4.78/70.4 (X_2), 5.08/71.4 (X_3), 5.39/68.2 (M_2), 4.24/62.4 and 4.36/62.4 ppm (M_6) are assigned to either xylose or mannose residues. Interpretation of the variation along the first component, t_1 , is straightforward and clearly shows that samples with positive values along t_1 , have higher cellulose contents at the expense of hemicelluloses compared to, for example, sample 10. This result is in good agreement with the carbohydrate composition determined by hydrolysis (Table 1) where dissolving pulps 2, 5, 7 and 8 were found to have the least amount of hemicelluloses and sample 10 was found to have the highest content of hemicelluloses. This is not contradicted by the models from the IR analysis.

In the second component, t_2 , samples from producer B stand out from the rest and are the only ones with positive values. These samples contain

more of the cell wall components resulting in positive peaks in the corresponding loading plot, Fig 4c. These positive peaks at 3.92/72.4, 4.69/97.5 and 5.39/68.2 ppm are due to mannose, and the most important negative peaks are the xylose peaks located at 3.35/62.1 and 3.96/62.1 ppm. This indicates that dissolving pulp from producer B has a higher mannose:xylose ratio than the other samples. This result is verified by the carbohydrate composition shown in Table 1.

OPLS-DA on process type

An OPLS-DA with the samples classified according to process type (sulfate or sulfite) resulted in a model with predictability of $Q^2 = 0.64$, with the score plot shown in Fig 5a. The corresponding loading plot (Fig 5c) shows that the most important negative peaks are the peaks from the reducing end of cellulose, C_{red} .

These are located at 5.69/91.31 and 6.28/88.6 ppm (Hedenström et al. 2009). Since observations from the sulfite process are negative in t_1 , Fig 5a, these samples have a relatively large proportion of reducing ends of cellulose.

A high value of reducing end groups (high copper number) corresponds well with a high amount of low molecular weight polysaccharides (Sixta et al. 2004). The spectra thus show that sulfite samples have a higher degree of reducing ends and hence a higher proportion of short cellulose chains compared to the sulphate pulps. This can also be seen in the distribution plots of the original pulps (not included), where all sulfite pulps have a hump at low molecular weights. This spectroscopic finding on reducing ends is also in agreement with results from wet chemical analysis, where sulfite pulps were found to have a higher fraction of low molecular weight cellulose, a higher level of reducing end groups (Sixta 2000) and a higher carbonyl content than sulfate pulps or cotton linters (Nagel et al 2005). The peaks in red at 4.53/80.3, 4.96/76.8, and 5.01/80.7 ppm have not been unambiguously assigned, but are only visible in the spectra from samples 9 and 10, both being the only samples where arabinose and galactose were detected by chemical analysis. These peaks are not as important in the models as the peaks from the reducing ends. The presence of these peaks in Fig 5c could be the result of the significantly higher hemicelluloses content for sample 9 and 10 and might thus not be related to the process type.

OPLS-DA on wood type

A second OPLS-DA was performed to investigate differences in the pulp samples related to the raw material used in the production, softwood or hardwood. This gave a model with a Q^2 of 0.40. In the

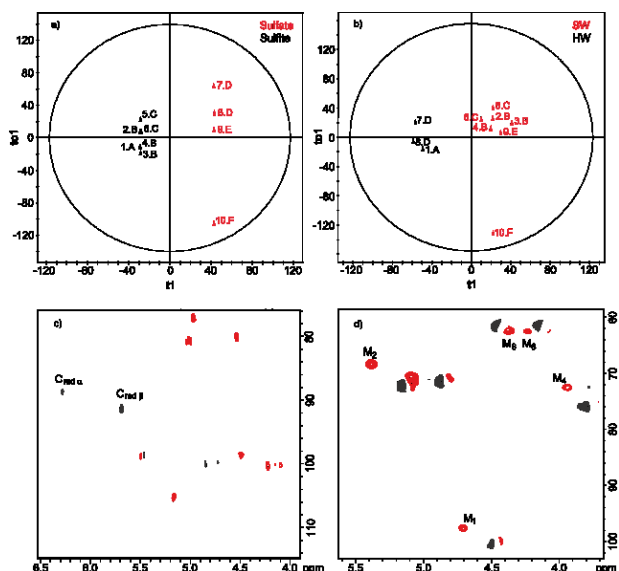


Fig 5. Plots from OPLS-DA models, calculated from 2D 1H - ^{13}C HSQC data, with sample classification according to either process type or wood type. Positive peaks are colored red and negative peaks are colored black, and only loadings with p-values above 0.5 are plotted in (c) and (d). (a) t_1 - t_01 score plot where samples were classified according to process type, sulfate or sulfite. (b) t_1 - t_01 score plot where samples were classified according to wood type, softwood or hardwood (c) Loading plot for the predictive component in a). Note that the area is zoomed to show only the most important peaks. (d) Loading plot for the predictive component in b).

score plot (Fig 5b) one could see that softwood samples are positive in t_1 . Peaks that are positive in the loading plot (Fig 5d) are mainly peaks from mannose, namely M2 (5.38/68.4), M1(7.72/97.3), M4 (3.94/72.6) and M6 (4.24 and 4.36/62.4). It can thus be concluded that the most important difference between the samples that correlate to raw material is that dissolving pulps produced from softwood have more mannose than pulp from hardwood. It is known that softwood contains more glucomannan than hardwood and it is clear that this difference in hemicelluloses composition is reflected in the final product. This result is in agreement with the "glycosidic" C-O-C vibrations found in the corresponding OPLS-DA models of the FT-IR data, because xylan is more branched than glucomannan.

As mentioned above, all samples were ball milled prior to the dissolution step of the samples. The effect of ball milling on the physical and chemical structure of cellulose is well known (Grohn 1958, Grohn, Deters 1962, Ott 1964, Schwanninger et al. 2004), mainly leading to a reduction of DP and a lower degree of crystallinity. However, ball milling has been found to be an essential step in the method for preparation of samples for analysis by 2D NMR (Hedenström et al. 2009, Lu, Ralph, 2003) and as such, the 2D NMR technique is included in this paper to detect possible correlations to pulp characteristics and conventional analytical methods. Despite ball milling, high correlations were found in

the presented models including high prediction ability for some important analytical methods.

Correlation between common cellulose analysis and spectroscopic methods

Correlations between common cellulose analysis and the spectroscopic methods used in this paper were investigated using OPLS or OPLS-DA models, see *Table 2*.

FT-IR spectra of the investigated dissolving pulps resulted in multivariate models for the analysis parameters Mn ($Q^2 = 0.75$), PD ($Q^2 = 0.64$), R10/R18 ($Q^2 = 0.46/0.63$), pore area ($Q^2 = 0.77$) and permeability ($Q^2 = 0.4$). For all these models the amount of hemicelluloses was the most important variable.

Solid-state ^{13}C NMR analysis gave good models for Mn ($Q^2 = 0.95$) and reasonable good models for R10/R18 ($Q^2 = 0.67/0.68$). For R10 and R18 the amount of hemicelluloses was the most important variable. For Mn, cellulose crystallinity is highly significant, where a high Mn value corresponds to a high crystallinity. 2D-NMR showed no correlation to Mn, which is obvious since Mn was shown to correlate to cellulose crystallinity that cannot be detected in solution. However, a good model was obtained for Mw ($Q^2 = 0.89$); an intriguing result since Mw was altered in the ball milling step. In the score plot one could see that viscosity is affecting the scores, where a higher value of Mw corresponds to a higher viscosity. The correlation between Mn with crystallinity and Mw with viscosity is highly interesting. The difference between Mn and Mw is a measure of the each sample's monodispersity. The closer the values become, the more monodisperse the cellulose chains become, resulting in more chains with similar DP values. We assume that cellulose with a larger fraction of uniform long chains tend to form more crystalline regions (perhaps by a "zipper" crystallization process) if the crystallization is not terminated by shorter chain molecules. Since Mn is the more varying descriptor in molecular weight distribution among the samples, it is thus the most significant variable in determining crystallinity. For R10/R18 ($Q^2 = 0.75/0.95$), hemicelluloses and the content of reducing end groups are most important. Permeability ($Q^2 = 0.48$) and pore area models ($Q^2 = 0.73$) confirm results from solid-state NMR, that the amount and nature of hemicelluloses is the most contributing factor for the prediction of those properties.

Interesting to note is the low predictability for R10/R18 by FT-IR, but high predictability by both NMR methods. The reason for that could be found in the method itself, where ATR FT-IR only analyses a region close to the surface of a sample,

Table 2. Overview of the correlations of all spectra to pulp origin and some analytical methods, and the predictive ability Q^2 of the models.

| Method | Discriminant | Q^2 |
|--------|--------------|-----------|
| FT-IR | Process type | 0.94 |
| FT-IR | Wood type | 0.76 |
| FT-IR | PD | 0.64 |
| FT-IR | Mn | 0.75 |
| FT-IR | Pore area | 0.77 |
| FT-IR | Permeability | 0.40 |
| FT-IR | R10/R18 | 0.46/0.63 |
| SS-NMR | Process type | 0.60 |
| SS-NMR | Mn | 0.95 |
| SS-NMR | R10/R18 | 0.67/0.68 |
| SS-NMR | Pore area | 0.64 |
| SS-NMR | Permeability | 0.48 |
| 2D-NMR | Process type | 0.64 |
| 2D-NMR | Wood type | 0.4 |
| 2D-NMR | R10/R18 | 0.75/0.95 |
| 2D-NMR | Mw | 0.89 |
| 2D-NMR | Pore area | 0.73 |
| 2D-NMR | Permeability | 0.48 |

instead of the whole sample such as for NMR analysis. Since the amount of hemicelluloses within the sample is not distributed homogeneously, FT-IR with ATR will be less accurate for the detection of hemicelluloses and the prediction of R10/R18 in contrast to NMR. Pore area, on the other hand, is a property derived from surface measurements and consequently should be well predicted by FT-IR for these samples. However, it comes as a surprise that Mn could be predicted by FT-IR ATR but not R18/R10, as both parameters reflect the average composition of the pulps. For a better predictability of R18/R10, the use of diffuse reflectance infrared FT spectroscopy could thus be of advantage.

An intriguing result of this study is that Mn and Mw can be predicted by both NMR methods, but no model could be achieved for intrinsic viscosity by any of the spectroscopic methods. Despite the intuition that Mn and Mw should correlate to intrinsic viscosity, the outcome of the models suggest that no such correlation exist. This result is strengthened by *Fig 6* where no correlation can be seen between Mv and Mw or Mn. Mv was derived from intrinsic viscosity by the Mark-Houwink equation using relevant coefficients for cellulose in cuen (Lojewski et al. 2010). Despite the importance of intrinsic viscosity as a qualitative analysis in industrial applications, both *Fig 6* (showing $R^2=0.662$ and $R^2=0.016$) and the models achieved suggest that no correlation exist between intrinsic viscosity and Mn or Mw supporting the results with models of high predictability for Mn and Mw but not intrinsic viscosity.

In addition, the influence of reducing end groups on pulp properties such as reactivity, peeling

(Hartler 1991), degradation under alkaline conditions and aging is well known (Nagel et al. 2005; Van Loon et al. 1999). Thus, a rapid spectroscopic measure of the degree of reducing end groups, instead of the conventionally used time-consuming wet chemical analysis, is of high importance for the pulp producer and consumer.

This also applies to the measurement of the xylose:mannose ratio, where xylose is known to be a major component of chemical-resistant hemicelluloses which undergo chemical association to cellulose, increasing the amount of the regenerative non-cellulosic material (beta-cellulose) and thus affecting for example the production of viscose filaments (Götze 1967). The presented 2D-NMR method combined with the OPLS-DA models presented in this study provide thus a future possibility to assign both a degree of reducing end groups and xylose:mannose ratios to unknown pulps, as described in the 2D-NMR analyses above. The models presented could thus help to predict, rather than replace, some of the complex analytical methods.

Table 3. Intrinsic viscosity and molecular weight of all samples investigated.

| | Viscosity (ml g ⁻¹) | Mv ^a (ml g ⁻¹) | Mw (ml g ⁻¹) | Mn (ml g ⁻¹) |
|----|------------------------------------|--|-----------------------------|-----------------------------|
| 1 | 587 | 203 346 | 485 500 | 39 647 |
| 2 | 465 | 156 967 | 397 154 | 50 075 |
| 3 | 573 | 197 964 | 383 647 | 47 922 |
| 4 | 845 | 304 813 | 520 837 | 57 961 |
| 5 | 423 | 141 295 | 354 086 | 51 650 |
| 6 | 785 | 280 861 | 477 154 | 59 647 |
| 7 | 516 | 176 208 | 358 058 | 78 542 |
| 8 | 609 | 211 831 | 514 295 | 106 288 |
| 9 | 419 | 139 811 | 292 104 | 50 368 |
| 10 | 794 | 284 442 | 483 635 | 60 448 |

^a calculated by Mark-Houwink equation where intrinsic viscosity $[\eta]=K \cdot Mv^a$, with $K=9.8 \cdot 10^{-3}$ and $a=0.9$ for cellulose solved in copper II ethylenediamine at 25 °C.

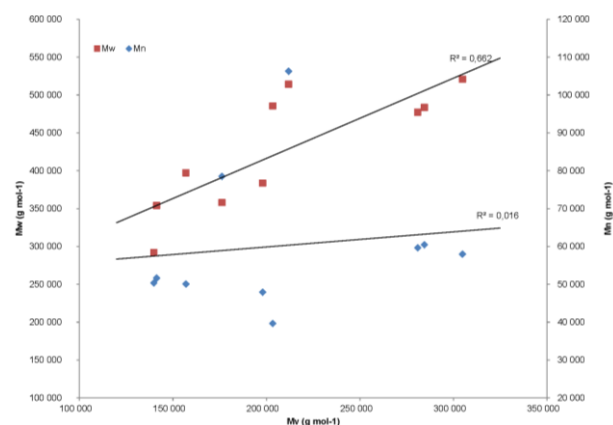


Fig 6. Correlation between Mv, derived from intrinsic viscosity, and Mw or Mn.

Conclusions

This study shows that FT-IR, solid-state ¹³C NMR and 2D ¹H-¹³C HSQC NMR spectra contain information that can be used to classify dissolving pulps according to their origin as well as their chemical and physical properties. The MVDA models obtained from these different spectroscopic methods can be used to classify unknown dissolving pulps samples to their origin in process type and wood type, but not with respect to viscosity. Here, models originating from 2D NMR and FT-IR could predict the pulps process type and wood type whereas solid state NMR distinguished between pulps from the various producers. Interpretation of the OPLS-DA models revealed that the main difference between softwood and hardwood pulp is the hemicelluloses composition, as also determined by the carbohydrate analyses. A C-O vibration band in the FT-IR spectra was found to be more prominent in spectra from hardwood pulp. If this is taken as an indication of a higher amount of branched polysaccharides, it could be related to the relatively higher intensities of the xylan peaks observed in the 2D NMR data and would then also be in agreement with the chemical analysis that shows that hardwood pulps contain a higher xylose:mannose ratio.

The 2D NMR data revealed a higher amount of reducing ends of the polysaccharide chains for sulfite pulp in comparison with sulfate pulp. This corresponds well to the higher fraction of short cellulose and hemicellulose chains of the sulfite samples as found by the molecular weight distribution measurements.

In addition, some of the spectroscopic methods provided measures of properties in pulps normally detected by more costly and time consuming analytical methods. R10, R18 and Mw or Mn could be predicted by FT-IR as well as by both solid state and liquid state NMR, while PD could only be predicted by FT-IR. Physical pulp properties such as permeability, pore area and pore diameter could also be predicted by the spectroscopic methods. In addition, Mn was found to correlate to crystallinity of the cellulose by solid state NMR, while Mw was highly correlated with pulp viscosity via 2D-NMR, indicating that the length of the molecular chains have an influence on crystallinity.

This is the first study where 2D NMR spectroscopy has been used to analyze dissolving pulp, and it is clear that this method is an interesting alternative to other techniques considering that MVDA type of interpretation of the spectra often is fast and straightforward, and that valuable information can be obtained. It has proven to have the potential to

give detailed information about hemicelluloses content as well as the existence and intensity of reducing ends in the cellulose chains - both very interesting parameters in the cellulose derivative manufacturing.

Acknowledgements

We would like to thank Funcfiber - A FORMAS center of excellence - for financial support. The support of the participating companies Domsjö Fabriker AB, AkzoNobel Functional Chemicals AB and Processum Biorefinery Initiative AB in Örnsköldsvik is gratefully appreciated. Thanks also to the staff at MoRe Research Örnsköldsvik AB for performing analyses or providing necessary equipment. A heartfelt thank you to Dr. Roland Agnemo for his support.

Literature

- Åkerholm, M., Salmén, L.** (2001): Interactions between wood polymers studied by dynamic FT-IR spectroscopy, *Polymer* 42 (3):963-969.
- Atalla, R.H., Gast, J.C., Sindorf, D.W., Bartuska, V.J., Maciel, G.E.** (1980): Carbon-13 NMR-spectra of cellulose polymorphs, *Journal of the American Chemical Society*, 102 (9):3249-3251.
- Barsberg, S.** (2010): Prediction of Vibrational Spectra of Polysaccharides - Simulated IR Spectrum of Cellulose Based on Density Functional Theory (DFT), *Journal of Physical Chemistry, B* 114 (36):11703-11708.
- Berthold, F., Gustafsson, K., Berggren, R., Sjöholm, E., Lindström, M.** (2004): Dissolution of Softwood Kraft Pulps by Direct Derivatization in Lithium Chloride/*N,N*-Dimethylacetamide, *Journal of Applied Polymer Science*, Vol. 94, 424-431.
- Byström, E., Viklund, C., Irgum, K.** (2010): Differences in porous characteristics of styrenic monoliths prepared by controlled thermal polymerization in molds of varying dimensions, *J. Sep. Sci.*, 33:1-9.
- Dudley, R.L., Fyfe, C.A., Stephenson, P.J., Deslandes, Y., Hamer, G.K., Marchessault, R.H.** (1983): High-Resolution ¹³C CP/MAS NMR Spectra of Solid Cellulose Oligomers and the Structure of Cellulose II, *Journal of the American Chemical Society*, 105 (8):2469-2472.
- Elg-Christoffersson, K., Sjöström, M., Edlund, U., Lindgren, Å., Dolk, M.** (2002): Reactivity of dissolving pulp: Characterisation using chemical properties, NMR spectroscopy and multivariate data analysis, *Cellulose*, 9, 159-170.
- Eriksson, L., Johansson, E., Wold-Kettaneh, N., Trygg, J., Wikström, C., Wold, S.** (2006) "Multi- and Megavariate Data Analysis, Part I, Basic Principles and Applications", *UMETRICS Academy*, (2): 95-98.
- Gerlach, R.W., Kowalski, B.R., Wold, H.O.A.** (1979): Partial least-squares path modelling with latent-variables, *Analytica Chimica Acta-Computer techniques and optimization* 3 (4):417-421.
- Grohn, H.** (1958): Über den mechanochemischen Abbau von Zellstoff durch Schwingmahlung. *Journal of Polymer Science*, vol. XXX (551-559), Prague Symposium.
- Grohn, H., Deters, W.** (1962): Über den mechanochemischen Abbau von Cellulose und Celluloseacetat durch Schwingmahlung. *Faserforschung und Textiltechnik*, 13, Heft 12 (544-549).
- Götze, K.** (1967): *Chemiefasern, Nach dem Viskoseverfahren*, Erster Band, Springer Verlag, Berlin, pp 118-120, 212-214.
- Hartler, N.** (1991): *Cellulose-technik*, Institutionen för cellulose-technik, Royal Institute of Technology, Stockholm. p 207-214.
- Hedenström, M., Wiklund-Lindström, S., Öman, T., Lu, F.C., Gerber, L., Schatz, P., Sundberg, B., Ralph, J.** (2009): Identification of lignin and polysaccharide modifications in populus wood by chemometric analysis of 2D NMR spectra from dissolved cell walls, *Mol Plant*, 2 (5):933-942.
- Hedenström, M., Wiklund, S., Sundberg, B., Edlund, U.** (2008): Visualization and interpretation of OPLS models based on 2D NMR data, *Chemometrics and Intelligent Laboratory Systems*, 92 (2):110-117.
- Hult, E.L., Larsson, P.T., Iversen, T.** (2000): A comparative CP/MAS ¹³C- NMR study of cellulose structure in spruce wood and kraft pulp, *Cellulose*, 7 (1):35-55.
- Immergut, E.H., Schurz, J., Mark, H.** (1953): Viskositätszahl-Molekulargewichts-Beziehung für Cellulose und Untersuchungen von Nitrocellulose in verschiedenen Lösungsmitteln, *Monatshefte für Chemie*, 84, 219-249.
- ISO 5351** (1981): Cellulose in dilute solutions- Determination of limiting viscosity number, International Organization for Standardization, 1st edition 19811201.
- ISO 699** (1982): Pulps- Determination of alkali resistance, International Organization for Standardization, 2nd edition 19821115.
- Isogai A., Usuda M., Kato T., Uryu T., Atalla R.H.** (1989): Solid-State CP/MAS ¹³C NMR study of cellulose polymorphs, *Macromolecules*, 22 (7):3168-3172.
- Iversen, T., Hult, E.L., Larsson, P.T., Wickholm, K.** (2000): CP/MAS C-13 NMR spectroscopy applied to structure studies on cellulose I, *Abstract of Papers of the American Chemical Society*, 219:U279-U279.
- Jackson, G.M., Mason, I.M., Greenhalgh, S.A.** (1991): Principal component transforms of triaxial recordings by singular value decomposition, *Geophysics*, 56 (4):528-533.
- Kačuráková, M., Capek, P., Sasinková, V., Wellner, N., Ebringerová, A.** (2000): FT-IR study of plant cell wall model compounds: pectic polysaccharides and hemicelluloses, *Carbohydrate Polymers*, 43 (2):195-203.
- KGI Securities Information** (2009): Viscose Fiber Sector, Quarterly Report, November 30, <http://research.kgi.com>, p5.
- Kim, H., Ralph, J., Akiyama, T.** (2008): Solution-state 2D NMR of ball-milled plant cell wall gels in DMSO-d(6), *Bioenergy Research*, 1 (1):56-66.
- Kono, H., Numata, Y.** (2004): Two-dimensional spin-exchange solid-state NMR study of the crystal structure of cellulose II, *Polymer*, 45 (13): 4541-4547.
- Kunze, J., Scheler, G., Schroter, B., Philipp, B.** (1983): ¹³C High-Resolution Solid-State NMR Studies on Cellulose Samples of Different Physical Structure, *Polymer Bulletin*, 10 (1-2):56-62.
- Labbé, N., Rials, T.G., Kelley, S.S., Cheng, Z.M., Kim, J.Y., Li Y.** (2005): FT-IR imaging and pyrolysis-molecular beam

mass spectrometry: new tools to investigate wood tissues, *Wood Science and Technology*, 39 (1):61-79.

Larsson, P.T., Hult, E.L., Wickholm, K., Pettersson, E., Iversen, T. (1999): CP/MAS ¹³C -NMR spectroscopy applied to structure and interaction studies on cellulose I, *Solid State Nuclear Magnetic Resonance* 15 (1):31-40.

Leclerc, D., Trung, T. (2002): Vibrational spectroscopy in the pulp and paper industry, Chalmers J, Griffiths P (eds) *Handbook of vibrational spectroscopy*, vol 4, John Wiley & Sons, Chichester.

Lojewski, T. Zieba, K., Lojewska J. (2010): Size exclusion chromatography and viscometry in paper degradation studies. New Mark-Houwink coefficients for cellulose in cupri-ethylenediamine, *Journal of Chromatography A*, 42: 6462-6468.

Lu, F.C., Ralph, J. (2003): Non-degradative dissolution and acetylation of ball-milled plant cell walls: high-resolution solution-state NMR. *The Plant Journal*, 35 (4):535-544.

Maréchal, Y., Chanzy, H. (2000): The hydrogen bond network in Iβ cellulose as observed by infrared spectrometry, *Journal of Molecular Structure*, 523:183-196.

Mohebbi, B. (2008): Application of ATR Infrared Spectroscopy in Wood Acetylation, *Journal Agric. Sci. Technology*, Vol. 10: 253-259.

Nagel, G., Potthast, A., Rosenau, T., Kosma, P., Sixta, H. (2005): Oxidation of Reducing End Groups in Cellulose According to Different Protocols, *Lenzinger Berichte*, 84:27-35.

Naumann, A., Navarro-Gonzalez, M., Peddireddi, S., Kues, U., Polle, A. (2005): Fourier transform infrared microscopy and imaging: Detection of fungi in wood. *Fungal Genetics Biology*, 42 (10):829-835.

Ott, R.L. (1964): Mechanism of the mechanical degradation of cellulose. *Journal of Polymer Science, A* (2):973-982.

Schwanninger, M., Rodrigues, J., Pereira, H., Hinterstoisser, B. (2004): Effects of short-time vibratory ball milling on the shape of FT-IR spectra of wood and cellulose. *Vibrational Spectroscopy* 36:23-40.

Sixta, H. (2000): *Lenzinger Berichte*, (79):119-128.

Sixta, H., Harms, H., Dapia, S., Parajo, J.C., Puls, J., Saake, B., Fink, H.-P., Röder, T. (2004): Evaluation of new organosolv dissolving pulps. Part I: Preparation, analytical characterization and viscose processability. *Cellulose*, 11: 73-83.

Široky, J., Blackburn, R.S., Bechtold, T., Taylor, J., White, P. (2010): Attenuated total reflectance Fourier-transform Infrared spectroscopy analysis of crystallinity changes in lyocell following continuous treatment with sodium hydroxide, *Cellulose*, 17:103-115.

Sjöholm, E. (1999): Characterization of Kraft pulps by Size-exclusion Chromatography, Doctoral Thesis, Royal Institute of Technology, Stockholm, Sweden, ISSN 1104-7003.

Stenlund, H., Gorzsás, A., Persson, P., Sundberg, B., Trygg, J. (2008): Orthogonal projections to latent structures discriminant analysis modeling on in situ FT-IR spectral imaging of liver tissue for identifying sources of variability, *Analytical Chemistry*, 80 (18):6898-6906.

Strunk, P., Eliasson, B., Hägglund, C., Agnemo, R. (2011): The influence of properties in cellulose pulps on the reactivity in

viscose manufacturing. *Nordic Pulp and Paper Research Journal*, 26(1):81-89.

Trygg, J., Wold, S. (2002): Orthogonal projections to latent structures (O-PLS), *Journal of Chemometrics*, 16 (3):119-128.

VanderHart, D., Atalla, R. (1984): Studies of Microstructure in Native Celluloses Using Solid-state ¹³C NMR, *Macromolecules*, 17:1465-1472.

Van Loon, L.R., Glaus, M.A., Laube, A., Stallone, S. (1999): Degradation of Cellulosic Materials Under the Alkaline Conditions of a Cementitious Repository for Low- and Intermediate-Level Radioactive Waste. *Journal of Environmental Polymer Degradation*, 7 (1):41-51.

Wickholm, K., Hult, E.L., Larsson, P.T., Iversen, T., Lennholm, H. (2001): Quantification of cellulose forms in complex cellulose materials: a chemometric model, *Cellulose*, 8 (2):139-148.

Wold, S., Esbensen, K., Geladi, P. (1987): Principal component analysis, *Chemometrics and Intelligent Laboratory Systems*, 2 (1-3):37-52.

Zhbankov, R.G., Korolevich, M.V., Derendyaev, B.G., Piottukh-Peletsy, V.N. (2005): Structural similarity and modeling of infrared spectra of molecules of organic compounds, *Journal of Molecular Structure*, 744:937-945.

Manuscript received May 20, 2011

Accepted August 8, 2011